ACS Pharmacology & Translational Science

pubs.acs.org/ptsci

Article

A Long-Acting Thermoresponsive Injectable Formulation of Tin Protoporphyrin Sustains Antitubercular Efficacy in a Murine Infection Model

Oluwatoyin A. Adeleke,* Logan Fisher, Ian N. Moore, Glenn A. Nardone, and Alan Sher

Cite This: *ACS Pharmacol. Transl. Sci.* 2021, 4, 276−287

Read Online

ACCESS | Metrics & More | Article Recommendations

ABSTRACT: Tuberculosis is the leading cause of death from a single infectious agent, ranking above the human immunodeficiency virus (HIV). Effective treatment using antibiotics is achievable, but poor patient compliance constitutes a major challenge impeding successful pharmacotherapeutic outcomes. This is often due to the prolonged treatment periods required and contributes significantly to the rising incidence of drug resistance, which is a major cause of tuberculosis mortality. Thus, innovative interventions capable of encouraging compliance and decreasing lengthy and frequent dosing are needed. Previously, aqueous tin protoporphyrin IX (SnPPIX), a heme oxygenase-1 inhibitor, administered as multiple daily intraperitoneal (IP) injections, showed considerable antitubercular efficacy and treatment shortening capabilities as a host-directed therapy in infected mice. Since daily IP injection is a clinically impractical administration approach, this proof-of-concept study aims to develop a novel, sustained action injectable formulation of SnPPIX for safe intramuscular (IM) administration. Herein, a SnPPIX-loaded poloxamer-poly(acrylic acid)-based thermoresponsive injectable formulation (SnPPIX-TIF) is designed for effective IM delivery. Results show SnPPIX-TIF is microparticulate, syringeable, injectable, and exhibits complete *in vitro*/*in vivo* gelation. Administered once weekly, SnPPIX-TIF significantly prolonged absorption and antimicrobial efficacy in infected mice. In addition, SnPPIX-TIF is well-tolerated *in vivo*; results from treated animals show no significant histopathologic alterations and were indistinguishable from the untreated control group, thus supporting its biocompatibility and preclinical safety. Overall, the IM delivery of the thermoresponsive injectable formulation safely sustains antitubercular effect in an infected murine model and decreases the number of injections required, signifying a potentially practical approach for future clinical translation.

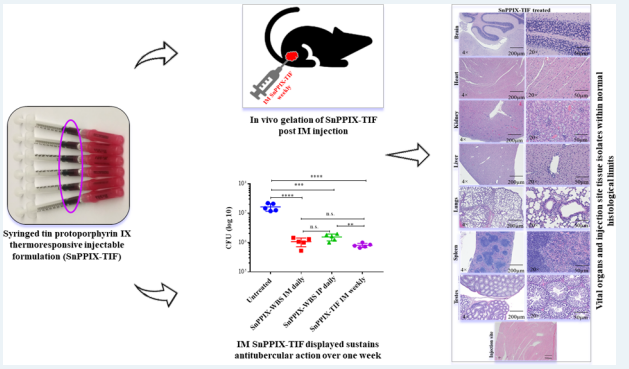

KEYWORDS: *tuberculosis, long-acting injectable, in situ forming polymeric gel, sustained drug delivery, host directed therapy, heme oxygenase-1 inhibitor*

1. INTRODUCTION

Tuberculosis (TB) remains one of the oldest known infectious diseases present in every country in the world. It is a major cause of human fatality, affecting all ages.[1−3] *Mycobacterium tuberculosis* (*Mtb*) is the etiologic agent of TB. In most cases, *Mtb* targets the lungs and rarely other body parts, leading to pulmonary and extrapulmonary infection, respectively.[3,4] Globally, it is one of the top 10 causes of death and leading cause from a single infectious agent, ranking above the human immunodeficiency virus (HIV)/acquired immune deficiency syndrome (AIDS), with ∼10 million new infections and 1.1−1.6 million fatalities annually (including HIV-positive individuals).[5−7] TB has been identified as a key cause of economic retardation, revolving poverty and illness that has entrapped families, societies, and even entire countries, with women, children, and HIV/AIDS patients being the most vulnerable.[8]

Most people who develop TB can be effectively cured and onward transmission can be curtailed with appropriate antibiotic treatment after diagnosis. However, poor patient compliance remains a major challenge impeding successful pharmacotherapeutic outcomes. This is often associated with the required lengthy treatment periods (≥6 months) and

Received: November 2, 2020
Published: December 18, 2020

https://dx.doi.org/10.1021/acsptsci.0c00185
ACS Pharmacol. Transl. Sci. 2021, 4, 276−287

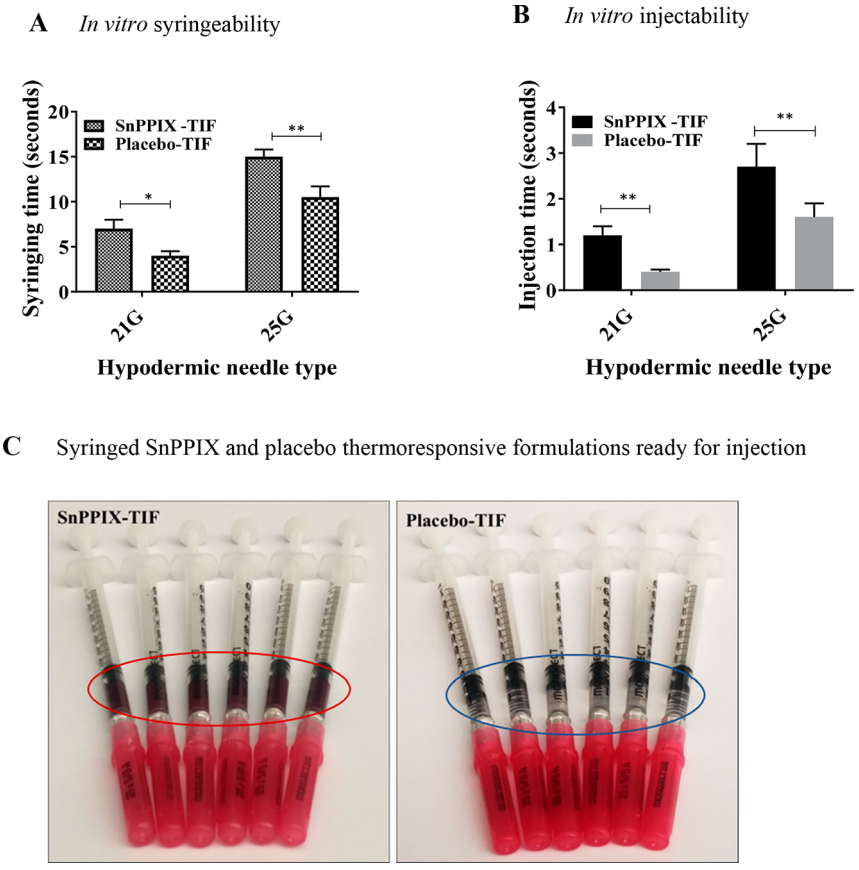

Figure 1. *In vitro/in vivo* syringeability and injectability of the SnPPIX and placebo thermoresponsive formulations. (A) Graphical representation of changes in *in vitro* syringing time, relative to the differences in needle size. (B) Charts comparing the disparities in injection time comparative to needle dimensions. (C) Respective digital photographs of the test formulations after syringing using a typical 25G needle in preparation for IM injection into the animal's rear leg thigh.

contributes significantly to the rising incidence of drug resistance, which is a major cause of TB mortality.[7,9,10] In an effort to address this problem, the WHO endorsed the administration of TB antibiotics three times weekly at clinics managed by designated health-care providers. This formed part of the directly observed treatment short course (DOTS) established in 1994.[10−12] Despite the reported relative effectiveness of this treatment approach, recent studies found that patients on the thrice weekly regimen were more susceptible to the development of drug resistance, indicating that a full treatment course may be more effective.[10,13,14] Moreover, the patient-care-centered WHO End/Stop TB strategy (built on the DOTS approach) further highlights the need for optimal use of currently available and other innovative tools, which can include new pharmaceutical actives and treatment regimens that can effectively support therapy, drug delivery ,and eventual disease eradication.[5,6,10] Measures such as electronic reminder devices, incentive programs, and simplified and shorter dosing regimens are being implemented to improve patient compliance and desired therapeutic effects.[15−17] Nevertheless, additional novel interventions capable of simplifying and shortening treatment periods, as well as promoting patient adherence, are still necessary to achieve global control and eradication of TB.

Recently, attention has focused on the potential of repurposing safe and well-tolerated therapeutic agents, many of which have broad immunomodulatory properties for use as adjunctive host-directed therapy (HDT) for TB management.[14,18−21] Host-directed therapeutic molecules are continuously researched and some are already in clinical trials, because of their identified capabilities to function as accelerators for conventional TB antibiotics or even treat multidrug resistant infections. HDT drugs are considered advantageous for achieving this purpose, because, unlike antibiotics, they generally act by targeting key immunomodulating host cell functions during the infectious process, rather than the pathogen itself. This thereby activates necessary immune defense mechanisms, which usually minimizes cell/tissue damage and does not promote the evolution of drug-resistant bacterial strains.[14,19−21] A candidate HDT drug previously investigated for TB chemotherapy was tin protoporphyrin IX (SnPPIX),[19] which is a heme oxygenase-1 inhibitor.[22−25] In prior experiments, SnPPIX administered as multiple daily intraperitoneal (IP) injections was reported to significantly decrease mycobacterial load as a monotherapy; moreover, when used in combination with conventional TB antibiotics, SnPPIX facilitated bacterial clearance and reduced treatment time by over one month in mice.[19]

Since the IP route of drug administration employed in the previous study is rarely used in humans and is minimally clinically acceptable or practical,[26,27] we reasoned that incorporating SnPPIX into a polymeric carrier for intramuscular (IM) delivery and staggered dosing could serve as a promising approach for safely improving its *in vivo* therapeutic performance and clinical applicability. Hence, we now report a proof-of-concept study where SnPPIX encapsulated in a

https://dx.doi.org/10.1021/acsptsci.0c00185
ACS Pharmacol. Transl. Sci. 2021, 4, 276−287

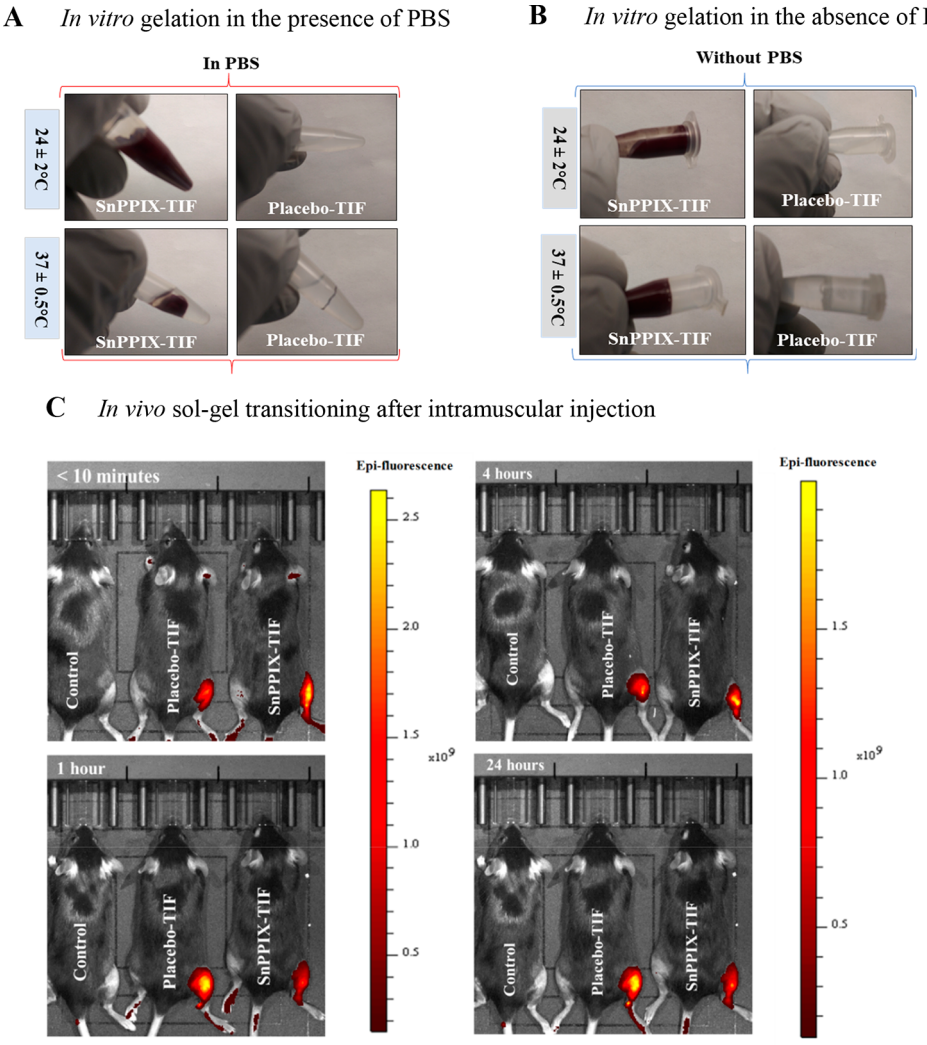

Figure 2. *In vitro* and *in vivo* sol−gel transitioning patterns of SnPPIX-TIF and placebo-TIF: (A) diagram showing formulation gelation into solid masses in the presence of PBS (pH 7.4) at 37 ± 0.5 °C; (B) illustration displaying congealed formulations at 37 ± 0.5 °C without PBS; and (C) image of anaesthetized mice exhibiting *in vivo* sol−gel changes upon IM injection of drug-loaded and placebo formulations, relative to the control animal that was not injected.

thermoresponsive injectable carrier, administered intramuscularly, sustains antitubercular efficacy in infected mice for 1 week. The thermally sensitive injection was designed by employing a blend of polyoxyethylene−polyoxypropylene−polyoxyethylene (Poloxamer) and a poly(acrylic acid) derivative. Poloxamers are biocompatible polymeric compounds that undergo temperature-dependent reversible gelation, which make them widely applicable as drug carriers for prolonged therapeutic effectiveness.[28−32] Conversely, poly(acrylic acid) polymers and their derivatives are nonthermosensitive biomaterials. They are vastly applied as mucoadhesive and dispersion stabilizing additives in medicinal products.[33,34] As described below, the physicochemical properties of the SnPPIX thermoresponsive injectable formulation (SnPPIX-TIF)—namely, gelation time, syringeability, injectability, particle size, and polydispersity index—were measured using *in vitro* methods. In addition, we investigated the pharmacokinetics and anti-TB efficacy of the SnPPIX-TIF *in vivo* and compared these with the conventional SnPPIX water-based solution (SnPPIX-WBS) administered either IP or IM. Finally, the tissue safety of the newly synthesized SnPPIX-TIF was systematically assessed by histopathologic examination of the injection sites, as well as vital organs. Our findings reveal SnPPIX-TIF as a safe and superior formulation for the administration of this HO-1 inhibitor as an HDT and provide an excellent example of the effective use of thermoresponsive polymers in drug delivery.

2. RESULTS AND DISCUSSION

2.1. Formulation Preparation. SnPPIX-TIF was prepared by employing the cold method coupled with direct encapsulation techniques. It appeared as a reddish-brown, uniformly dispersed colloidal mix that remained liquid under room-temperature (23 ± 2 °C) and refrigerated (2−8 °C) conditions but rapidly congealed at ∼37 ± 0.5 °C. The placebo-TIF, on the other hand, is presented as a clear colloidal solution that displays similar (to the SnPPIX-TIF) solid−liquid phase transitioning at room temperature, as well as refrigerated and physiological temperatures. The SnPPIX-WBS was also reddish-brown in color but was an aqueous solution, which elicited no temperature-dependent phase changes.

2.2. Physicochemical Characteristics. *2.2.1. Syringe Filling and Emptying−In Vitro and In Vivo Evaluations.*

https://dx.doi.org/10.1021/acsptsci.0c00185
ACS Pharmacol. Transl. Sci. 2021, 4, 276−287

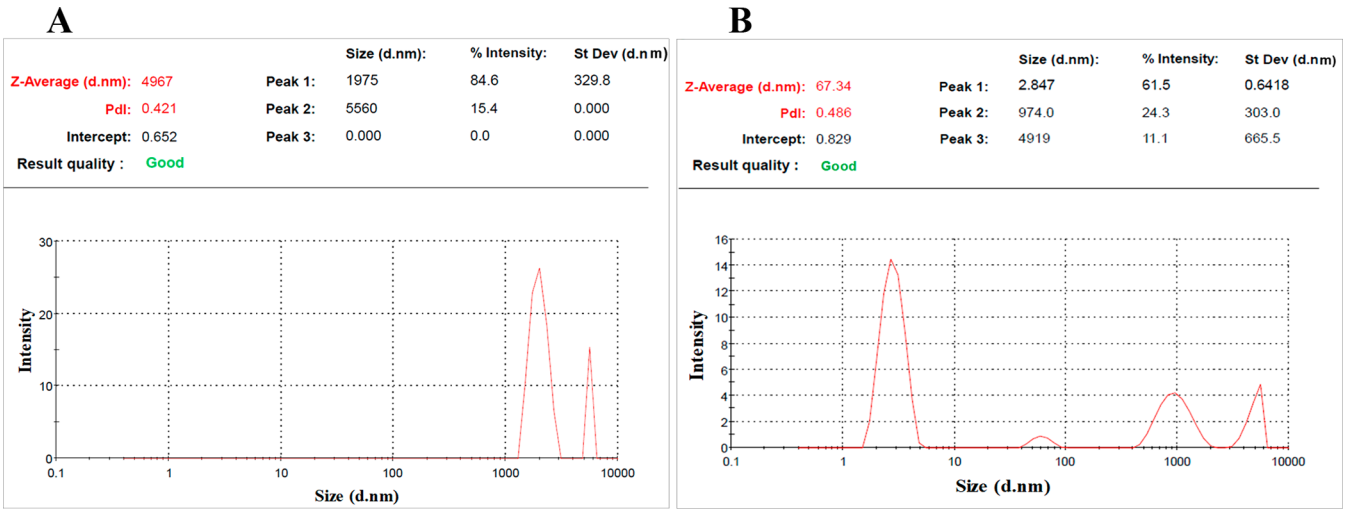

Figure 3. Characteristic particle sizing and distribution pattern for the (A) SnPPIX-TIF and (B) placebo-TIF retrieved from the Malvern Zetasizer report.

Syringeability and injectability experiments were performed manually *in vitro* under ambient conditions (24 ± 2 °C), using two different hypodermic needle types (21G and 25G) to evaluate the effects of diameter and length on the injection time by keeping the test substance, volume, and plunger displacement comparatively constant. For each 0.1 mL of SnPPIX-TIF or placebo-TIF, the recorded syringing time (for SnPPIX-TIF: 21G = 7.0 ± 1.0 s and 25G = 15.0 ± 0.8 s; for Placebo-TIF: 21G = 4.0 ± 0.5 s, and 25G = 10.5 ± 1.2 s) (Figure 1A) and injection time (SnPPIX-TIF: 21G = 1.2 ± 0.2 s, and 25G = 2.7 ± 0.5 s; Placebo-TIF: 21G = 0.4 ± 0.1 s, and 25G = 1.6 ± 0.3 s) (Figure 1B) were rather minimal. However, for both tests involving the 21G and 25G needles, more time was needed to syringe the drug formulation (SnPPIX-TIF) than to inject or eject it, compared to its placebo counterpart. The presence of the SnPPIX molecules within the polymeric network appeared to trigger a level of resistance to flow that slowed both the syringing and injection processes, evidenced by the documented difference in the time elapsed. On the other hand, the placebo-TIF was easier to manipulate through the syringe and needle passages, as indicated by a decrease in measured time, presumably because friction-bearing SnPPIX molecules were absent within the formulation matrix.

The length of time needed to transfer 0.1 mL SnPPIX-TIF or placebo-TIF via the syringe-needle assembly (Figure 1C) to the IM tissue space located within the rear leg thighs of the mouse model was logged as *in vivo* injectability. Since the 25G needles exhibited longer injection times (which is an indication of resistance to flow) for both SnPPIX-TIF and placebo-TIF, it was selected as a suitable prototype for testing the injectability of these formulations *in vivo*. Utilizing the 25G needle, the documented *in vivo* injection times were 2.8 ± 1.2 s and 1.3 ± 0.4 s for the SnPPIX-TIF and placebo-TIF, respectively. These findings followed the same trend observed for the *in vitro* specimens, in which case the placebo formulation (drug free) required less injection time, compared to its drug-loaded counterpart. Both *in vitro* and *in vivo* experiments reported at this juncture show that, overall, both placebo and SnPPIX-loaded formulations responded reasonably well, as a function of the time elapsed, during the syringing and injection processes.

2.2.2. In Vitro and In Vivo Gelation. *In vitro* gelation patterns were studied for the placebo-TIF and SnPPIX-TIF under biorelevant conditions (PBS, pH 7.4, and 37 ± 0.5 °C) in a digital water bath employing the earlier described tube inversion technique. With or without PBS, both samples formed completely gelled solid masses *in vitro* under 30 s (Figures 2A and 2B). In PBS, the recorded gelation times were 18.12 ± 1.71 s and 21.78 ± 3.24 s for the placebo-TIF and SnPPIX-TIF, respectively. In the absence of PBS, the placebo-TIF congealed at 23.01 ± 1.14 s and SnPPIX-TIF at 28.67 ± 0.58 s. In both instances (i.e., with and without PBS), the SnPPIX-TIF required slightly more time to congeal than the placebo formulation, which may be attributable to the presence of the drug molecules within the polymeric carrier network.

After IM injection of 0.1 mL SnPPIX-TIF or placebo-TIF into the thigh muscle of the right hind limb using a 25G needle, each formulation exhibited sol-to-gel alteration at body temperature by forming a defined, localized fluorescing solid mass that appeared intact at the injection site, rather than spreading to form a sheetlike geometry (Figure 2C). The structure of the mass produced *in vivo* was maintained at the time points when it was visualized. The formation of a compact gel network *in vivo* under 10 min after IM injection indicated that the sol−gel transitioning process was rapid and the persistent appearance of the fluorescing gelled mass at 1, 4, and 24 h post-injection supports its controlled dissolution and sustained activity behavior. Our findings show that the thermoresponsive formulation developed in this study is potentially ideal for designing an injectable drug delivery system in which case production and administration can occur under ambient conditions while solidified gel formation only happens at body temperature.

2.2.3. Particulate Sizing and Distribution. The mean particle size, distribution, and polydispersity index (PDI) of pharmaceutical formulations meaningfully influence physical properties, stability, and *in vivo* activity of colloidal dispersion systems. For this reason, controlling these parameters represents an important variable in the formulation development process.[42,43] The average hydrodynamic particle size for the respective populations and PDI were 4967.00 nm and 0.42, respectively, signifying that the SnPPIX-TIF was largely microstructured and relatively evenly dispersed. Identified

https://dx.doi.org/10.1021/acsptsci.0c00185
ACS Pharmacol. Transl. Sci. 2021, 4, 276−287

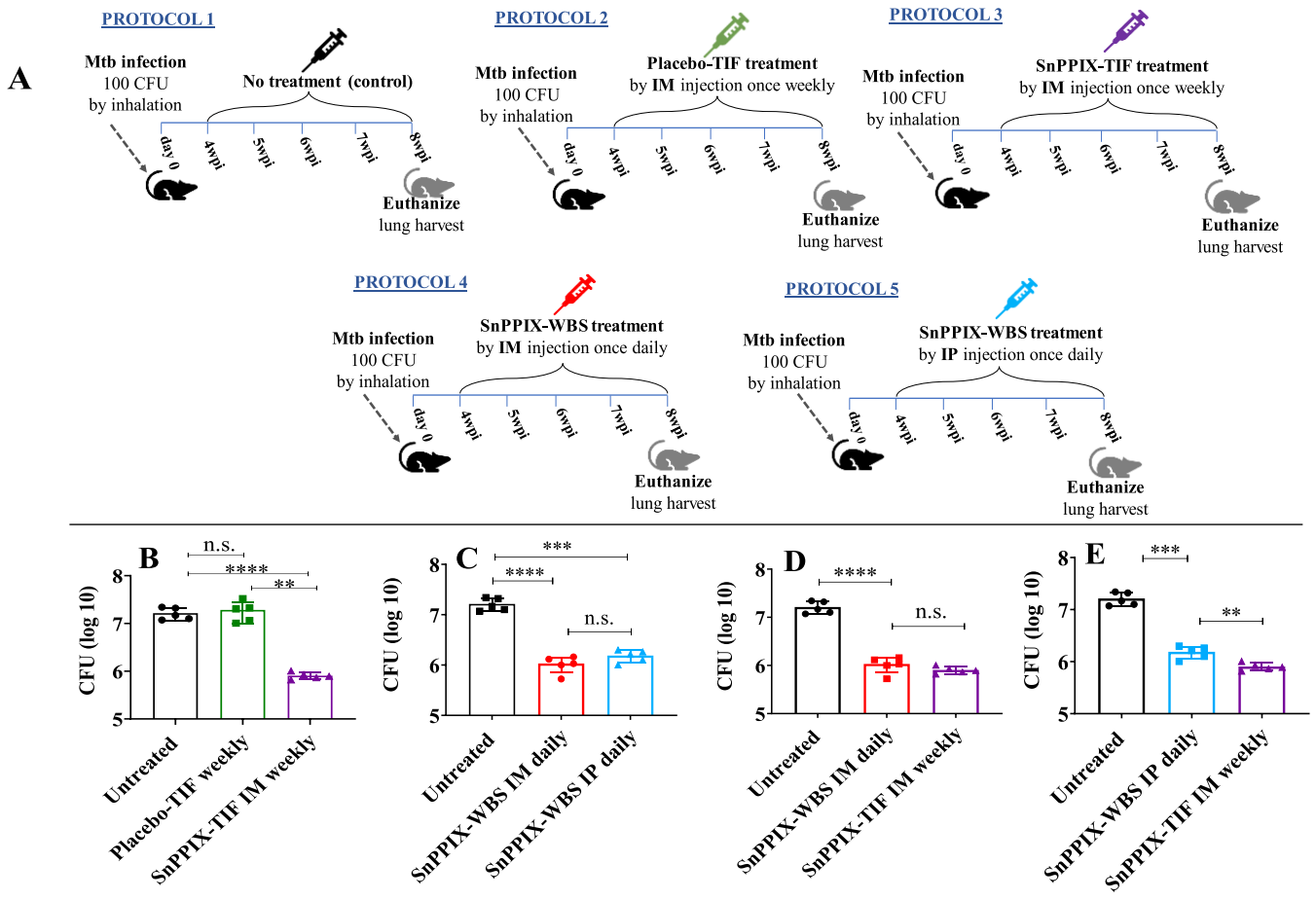

Figure 4. Polymer-based SnPPIX (SnPPIX-TIF) administered weekly by the IM route to *Mtb* infected mice induces highly significant reductions in bacterial loads, comparable to water-based SnPPIX (SnPPIX-WBS) given daily via IP or IM injection. (A) Illustration of the different experimental protocols employed for the infection, treatment, and control (untreated and placebo-treated) mouse groups. (B−E) Comparative evaluation of lung mycobacterial loads among untreated and treated animals, based on the SnPPIX preparations/regimens or placebo-TIF used for each experimental condition. [Statistical disparities were considered significant when (*) $p \leq 0.05$, (**) $p \leq 0.01$, and (***) or (****) $p \leq 0.0001$; meanwhile, "n.s." denotes nonsignificance. Representative outcomes of 2−3 independently performed experiment are shown in each panel.]

particle populations were mainly in two categories, with ∼85% being 1975.00 nm and smaller in size and the remaining ∼15% were 5560.00 nm and less (Figure 3A). The placebo-TIF was instead largely nanoparticulate in nature, with a PDI of 0.49 and a mean hydrodynamic particle size of 67.34 nm with population distribution outlined as ∼62% characterized by sizes of ≤2.85 nm, ∼24% showing sizes of ≤974.00 nm, and ∼11% having diameters of ≤4919.00 nm (Figure 3B). Focusing on the average hydrodynamic size of 67.34 nm, the placebo-TIF generally had smaller particle sizes, compared to the Sn-PPIX-TIF (4967.00 nm), indicating that the SnPPIX molecules were loaded onto the thermoresponsive polymeric carrier matrix, forming larger microconfigured units.

The presence of more than one particle population (based on size) for both drug and placebo formulations indicate that there is a level of interparticle aggregation occurring within these hydrogel carrier matrices. This is not unexpected, considering the temperature-dependent sol−gel transitioning properties of the polymeric thermoresponsive template employed in the fabrication of the placebo-TIF and SnPPIX-TIF. This inference is further supported by the slightly higher PDI value obtained for the placebo-TIF (0.49), relative to that of the SnPPIX-TIF (0.42). In addition, the SnPPIX-TIF had two particulate populations while the placebo-TIF presented three categories, based on the enumerated particle dimensions. This indicates that the SnPPIX formulation appeared to accumulate at a slower rate, forming fewer particle agglomerates, relative to its drug-free analogue. The latter outcome relates well to the earlier-described gelation time values, whereby the drug formulation required longer time frames to congeal under higher-temperature *in vitro* conditions. Knowledge of the particle size distribution for drug formulations is critical in ensuring that batch-to-batch consistency is maintained throughout the development process.[44,45]

2.3. Antitubercular Efficacy of SnPPIX-TIF *In Vivo*. As introduced above, SnPPIX was formerly shown to induce highly significant antitubercular efficacy against *Mtb*, when administered to infected mice alone and when combined with conventional first-line TB antibiotics, reduced treatment duration for over one month.[19] However, in these experiments, SnPPIX was administered as a daily water-based IP injection over an extended period, which is an approach that would be clinically impractical.[26,27] As a means for overcoming this limitation, we explored the use of the poloxamer−poly(acrylic acid) polymer-based thermoresponsive flexible matrix described above as a biocompatible injectable carrier for SnPPIX (i.e., SnPPIX-TIF) to achieve sustained antitubercular efficacy

https://dx.doi.org/10.1021/acsptsci.0c00185
ACS Pharmacol. Transl. Sci. 2021, 4, 276−287

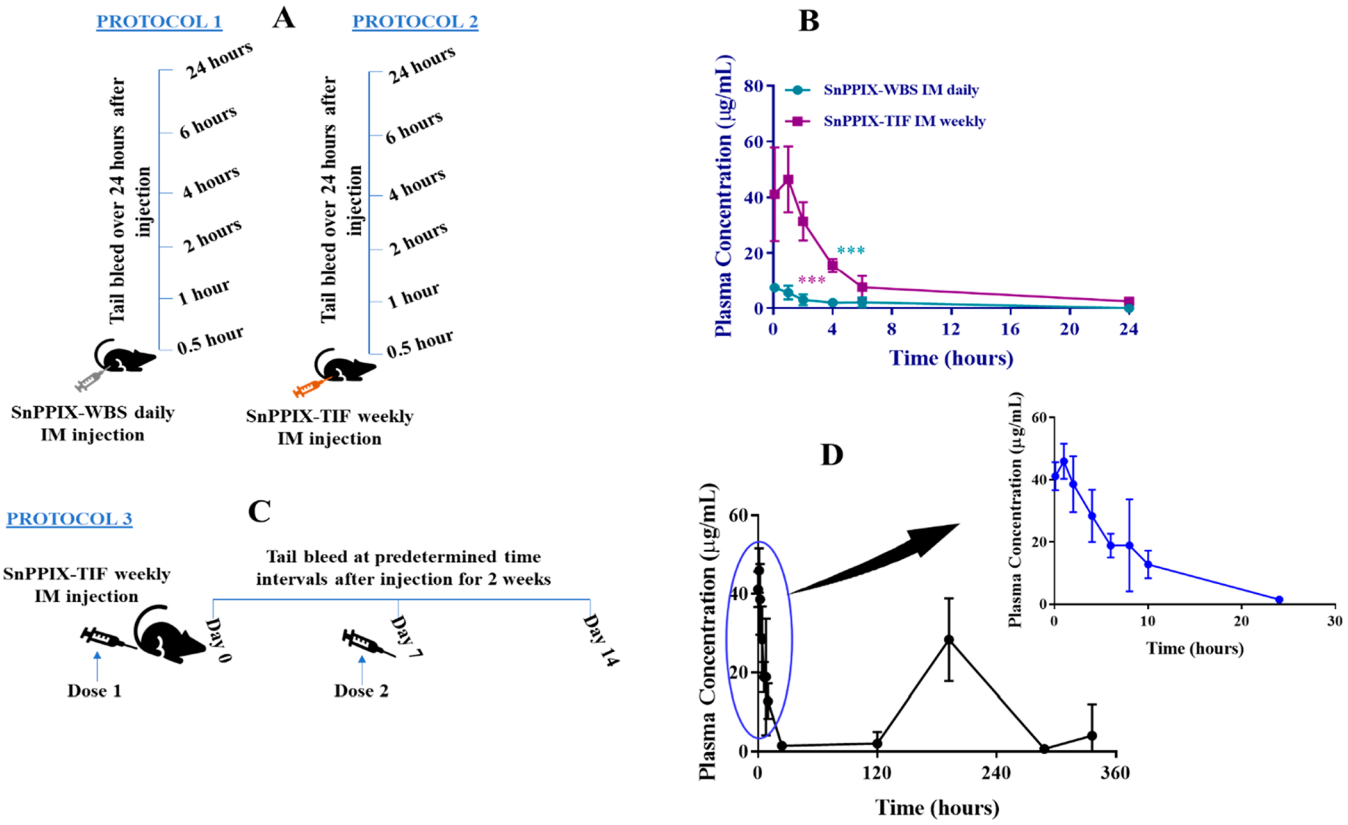

Figure 5. Plasma pharmacokinetics of SnPPIX from the water-based and thermoresponsive polymer-based preparations. (A) An illustration of the 24-h treatment protocol for single-dose SnPPIX-WBS or SnPPIX-TIF IM injection. (B) Graphical representation comparing the changes in SnPPIX plasma concentrations at specific time intervals. (C) Diagram of experimental procedure implemented for evaluating the extended drug release behavior of the injected SnPPIX-TIF. (D) Sustained drug plasma concentration−time profile after administering the SnPPIX-TIF once weekly for a total of two weeks. Data points represent mean values, and error bars represent standard deviations; n = 5 mice per experiment.

via IM delivery with less frequent dosing, which is a more clinically acceptable drug administration technique. To evaluate the impact of each treatment scheme on the lung *Mtb* bacterial burden following inhaled low dose infection, SnPPIX, placebo-treated and untreated animals were utilized. Pulmonary mycobacterial loads were determined by culture at the end of each experimental protocol (Figure 4A). To determine whether the newly developed SnPPIX-TIF weekly IM injection showed extended antitubercular effectiveness, we compared the reduction in pulmonary mycobacterial load achieved with treatment protocols involving conventional daily water-based SnPPIX IM or IP injections in infected mouse groups, relative to the untreated control animals.

We observed that weekly IM injections of the SnPPIX-TIF for 4 weeks significantly reduced pulmonary mycobacterial load in infected mice indicating that encapsulating SnPPIX within the thermoresponsive, sustained release polymeric carrier platform did not impede its antimicrobial activity (Figure 4B). The mean bacterial CFU loads in the IM SnPPIX-TIF-treated cohort (5.8 logs) were significantly ($p \leq 0.0001$) lower than the average values recorded for the untreated *Mtb* infected animals (7.2 logs) or placebo-TIF treated (7.4 logs) animal groups. Consistent with previous findings, the water-based SnPPIX daily injection (SnPPIX-WBS) given IP (6.2 logs) or IM (6.0 logs) also significantly ($p \leq 0.01$) reduced mycobacterial levels, relative to that of the untreated controls (7.2 logs). Moreover, treatment with IM placebo-TIF weekly (7.4 logs) did not significantly reduce bacterial burden, when compared to the untreated control group (7.2 logs), indicating that the antitubercular effect observed with weekly IM SnPPIX-TIF was directly attributable to the presence of the active drug molecules (Figure 4B). Interestingly, the differences in the administration routes had no statistically relevant influence on the resulting antibacterial activity of each protocol (Figure 4C). Furthermore, the antimicrobial efficacy of the SnPPIX-TIF delivered intramuscularly once weekly was identical to the daily SnPPIX-WBS IM injections (Figure 4D) but was noticeably ($p \leq 0.01$) better than that of the daily SnPPIX-WBS IP injections. Importantly, the IM SnPPIX-TIF treatment given at weekly intervals resulted in a reduction in pulmonary bacterial loads of over a one log, comparable to that achieved with daily IM and superior to that attained by daily IP SnPPIX-WBS injections.

2.4. Tin Protoporphyrin Pharmacokinetics. Based on the above results, we hypothesized that the inclusion of SnPPIX into an IM injected thermoresponsive poloxamer−poly(acrylic acid) polymeric carrier meaningfully sustained its antimicrobial effect. To support these findings, we first attempted to monitor changes in SnPPIX plasma concentration over 24 h following single dose SnPPIX-WBS or SnPPIX-TIF preparations given via the IM route. IM SnPPIX-WBS was selected over its IP counterpart, because of its significantly enhanced antimicrobial effect (Figure 4C). The experimental procedure used and the plasma concentration versus time profile are presented in Figures 5A and 5C, respectively. The drug displayed rapid absorption for both injections and was detected in plasma within 30 min post-administration. No drug remained detectable 10 h following

https://dx.doi.org/10.1021/acsptsci.0c00185
ACS Pharmacol. Transl. Sci. 2021, 4, 276−287

SnPPIX-WBS injection, while it persisted at low but traceable levels for 24 h in the SnPPIX-TIF injected mice (Figure 5B). Overall, the SnPPIX-TIF treatment significantly enhanced drug absorption as it was presented with significantly higher AUC_{0-24} (575.1 ± 38.5 μg h/mL), maximum plasma concentration (C_{max} = 46.5 ± 11.8 μg/mL), C_{max} time (t_{max} = 1 h), and half-life ($t_{1/2}$ = 2.77 h). In contrast, the daily SnPPIX-WBS injection was also absorbed *in vivo* but had a lower AUC_{0-24} = 38.8 ± 4.4 μg h/mL; C_{max} = 7.4 ± 1.6 μg/mL, t_{max} = 0.5 h, and $t_{1/2}$ = 1.89 h (see Table 1). Of note, all animals maintained normal eating and drinking behavior and appeared healthy during and after the experiment. In summary, SnPPIX encapsulation into the thermoresponsive polymeric carrier (i.e., SnPPIX-TIF) notably delayed and improved drug absorption, as evidenced by higher t_{max}, AUC_{0-24}, and C_{max} numerical values.

Table 1. Tin Protoporphyrin Plasma Concentration (Mean ± SD) Changes over Time for the SNPPIX-TIF and SnPPIX-WBS IM Injections[a]

parameter[b]	Value	
	SnPPIX-TIF	SnPPIX-WBS
AUC_{0-24}	575.10 ± 38.51 μg h/mL	38.80 ± 4.40 μg h/mL
C_{max}	46.50 ± 11.80 μg/mL	7.40 ± 1.60 μg/mL
t_{max}	1.00 h	0.50 h
$t_{1/2}$	2.77 h	1.89 h

[a] n = 5 mice per experimental group. [b] AUC = area under the plasma concentration−time curve, C_{max} = maximum plasma concentration, t_{max} = time needed to reach maximum levels, and $t_{1/2}$ = time needed to reach half-life. Generated values were within the limit of quantification of the fluorometer.

To further visualize the extended pharmacokinetics of the newly designed SnPPIX-TIF, additional animal groups (n = 5 each) were given 0.1 mL IM injections (5 mg/kg) once weekly for two weeks (Figure 5C). Detection of SnPPIX in plasma occurred as early as 30 min and *in vivo* drug release/absorption from the polymeric carrier was relatively delayed. SnPPIX plasma absorption predominantly occurred within 24 h post-administration (same trend observed for the two doses given) with reasonably low plasma levels being maintained over prolonged periods (Figure 5D). Interestingly, antimicrobial efficacy was still maintained, even at this low SnPPIX plasma, as evidenced by the consistent reduction in bacterial load (relative to the SnPPIX-WBS) described above (see Figures 4D and 4E). The ability of the polymer-based thermoresponsive carrier to contain and function as an effective SnPPIX depot intramuscularly complements scientific efforts to fabricate smart, long acting bioactive injectables that can potentially promote dose spacing and patient compliance. Further optimization of SnPPIX *in vivo* absorption such that drug plasma concentrations are maintained at levels that can improve antitubercular efficacy appears to be an important next step.

2.5. Preclinical Safety Evaluation Using Histopathological Methods. General toxicity examinations were performed by comparing the effects of treating mouse groups (n = 3 in each case) with SnPPIX-TIF or placebo-TIF once weekly with the untreated control group for a total of four weeks. All vital organ tissue specimens (i.e., heart, kidney, lungs, liver, brain, testes, spleen), including the injection site muscle tissue collected from the treated (i.e., with drug and placebo formulations) and untreated control mice cohorts at the end of the four-week investigation, received a score of "0". These tissues were found to be within normal histologic limits. Overall, the newly designed SnPPIX-TIF and drug-free placebo-TIF were well-tolerated *in vivo*, and results from treated animals showed no significant histopathologic alterations and were indistinguishable from the untreated control group, thus supporting their biocompatibility and lack of toxicity. Representative photomicrographs for all tested vital organ (Figure 6A) and injection site muscle tissue (Figure 6B) specimens are presented in Figure 6.

3. METHODS

3.1. Materials. Tin protoporphyrin IX, deuteroporphyrinIX-2,4-disulfonic acid, and 10% neutral buffered formalin were purchased from Frontier Scientific (Logan, UT, USA) and RICCA Chemical Company (Arlington, TX, USA), respectively. Gibco Dulbecco's Phosphate-Buffered Saline (DPBS) was obtained from Life Technologies Corporation (Grand Island, NY, USA). Phosphate buffered saline (PBS), 45% sodium polyacrylate solution, poloxamer 407, hematoxylin and eosin (H&E) stain, acetonitrile, dimethylformamide, 4-morpholineethanesulfonic acid, methanol, sodium hydroxide, hydrochloric acid, 7H9 and 7H11 media were obtained from Sigma−Aldrich Chemical Co. (St Louis, MO, USA). Glycerol and oleic acid-albumin-dextrose-catalase (OADC) were procured from Mallinckrodt Pharmaceuticals (Staines-Upon-Thames, Surrey, U.K.) and BD Biosciences (Billerica, MA, USA), respectively. Tween 80 was purchased from Thermo Fisher Scientific (Washington, DC, USA).

3.2. Preparation of Placebo, SnPPIX Thermoresponsive Formulations, and SnPPIX Water-Based Solution. The drug-free blend of poloxamer−poly(acrylic acid) polymeric blend herein referred to as placebo thermoresponsive injectable formulation (placebo-TIF) was prepared by employing the "cold method".[34−36] Poloxamer powder was dispersed in 10 mL of deionized water containing 0.1 g sodium polyacrylate solution that was occasionally mixed until the solute particles were completely dissolved and a clear homogeneous solution formed. Thereafter, the SnPPIX thermoresponsive injectable formulation (SnPPIX-TIF) was developed by directly encapsulating SnPPIX powder calculated as a standard dose of 5 mg/kg per mouse[19] into the placebo-TIF mixture under continuous mechanical stirring (ULTRA-TURRAX Tube Drive Control Disperser, IKA Works, Inc., Wilmington, NC, USA) until complete incorporation was achieved and a monophased, colloidal mixture formed. Lastly, the conventional SnPPIX water-based solution (SnPPIX-WBS) was made by dissolving SnPPIX (5 mg/kg) in 0.1 M aqueous NaOH, then diluting in phosphate buffered saline (PBS) and adjusting pH to a neutral range (7.0−7.4), using 0.1 M hydrochloric acid. The resulting placebo-TIF, SnPPIX-TIF and water-based solution were stored in the refrigerator (−4 ± 2 °C) for subsequent *in vitro* and *in vivo* testing.

All SnPPIX and placebo preparations planned for parenteral administration (IM and IP routes) to the different mice cohorts were prepared using sterile water suitable for injection and filtered through a sterile, 0.22 μm Whatman cellulose acetate membrane syringe filter (Cytiva, MA, USA). All materials required for this processes were handled in a biosafety cabinet, employing standard precautionary measures.

3.3. Measured Physical Properties. *3.3.1. Syringeability and Injectability.* *Syringeability* refers to the ease of

https://dx.doi.org/10.1021/acsptsci.0c00185
ACS Pharmacol. Transl. Sci. 2021, 4, 276−287

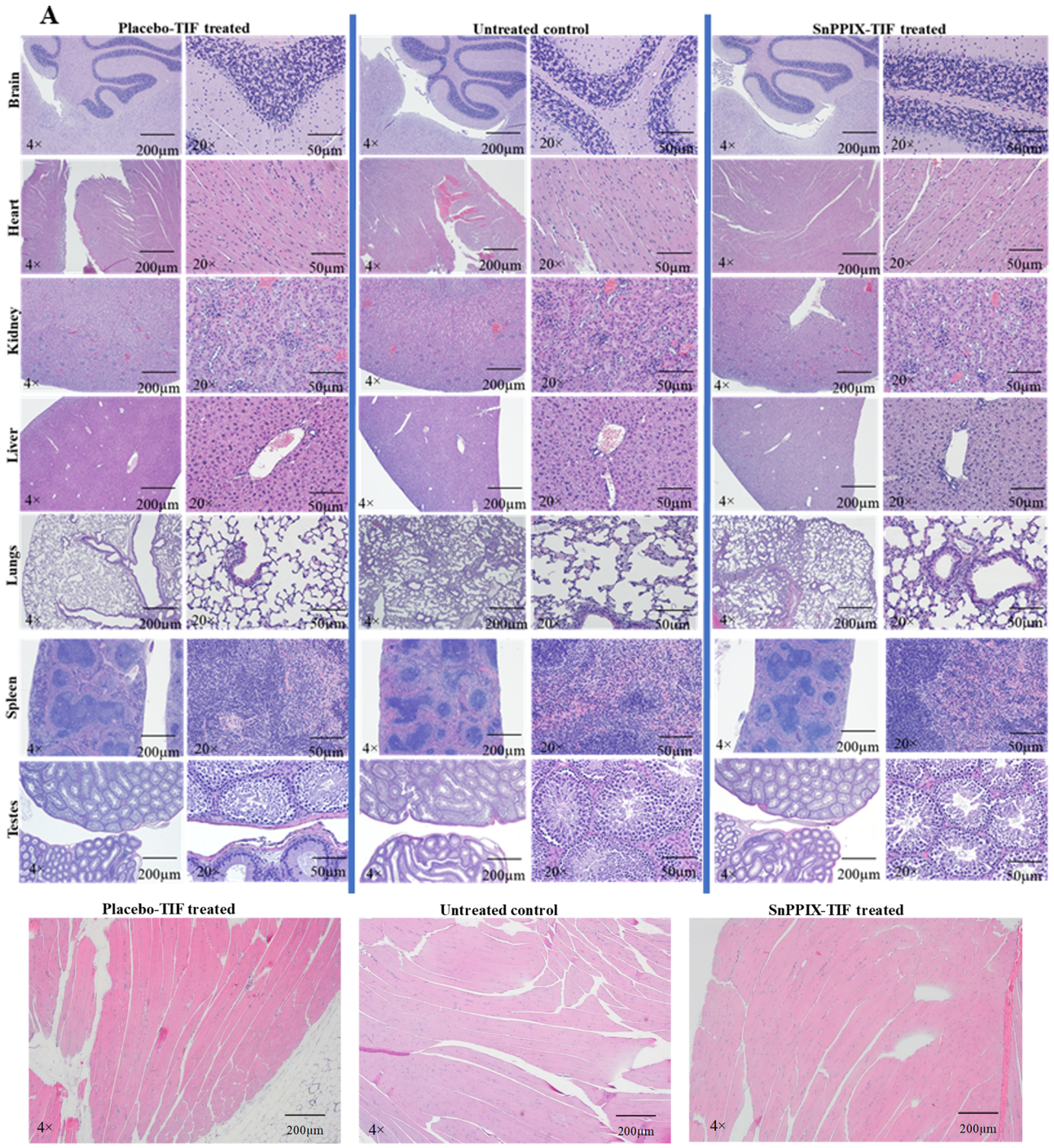

Figure 6. Representative photomicrographs of (A) vital organ tissues obtained from untreated and treated (SnPPIX-TIF and placebo-TIF) animals and (B) rear thigh muscle collected from the injection site for both SnPPIX-TIF and placebo-TIF after four weeks. Images were captured at 4× and 20× magnifications.

formulation withdrawal from a vial through a needle into the syringe while *injectability* describes formulation transfer from the syringe via the needle to the administration site during injection activities. These parameters are important functions of the needle−syringe−formulation combined systems and must be carefully considered when designing injectable drug formulations, because they determine the force of injection, which directly impacts inoculation duration, pain, discomfort, patient retention, and compliance.[37−40] In this case, syringeability and injectability were measured *in vitro* as the time required for 0.1 mL of SnPPIX-TIF or placebo-TIF to be manually transferred from the vial into the syringe or during injection into the body, respectively. Syringe plunger displacement was manually executed by the same individual to minimize fluctuations in injection rate or manually applied force. Tests were performed under ambient conditions (24 ± 2 °C). Monoject syringes (1 mL) were equipped with 21G (diameter = 0.80 mm and length = 25.00 mm) BD PrecisionGlide (BD Company, NJ, USA) or 25G (diameter = 0.51 mm and length = 16.00 mm) Monoject hypodermic conventional needles (Covidien LLC, MA, USA). Five replicate readings were recorded for each testing condition,

https://dx.doi.org/10.1021/acsptsci.0c00185
ACS Pharmacol. Transl. Sci. 2021, 4, 276−287

using a West Bend electronic timer. The 25G hypodermic needle was employed for subsequent *in vivo* studies, considering its narrower inner diameter, which would further validate injectability assessments in the mouse model.

3.3.2. In Vitro Gelation Time. *In vitro* gelation time was measured as the period required for the SnPPIX-TIF or placebo-TIF to congeal post-exposure to a temperature of 37 ± 0.5 °C, mimicking physiological conditions. First, gelation time was determined in the absence of PBS using the tube inversion approach.[15,34] Briefly, 500 μL of the SnPPIX-TIF or placebo-TIF was transferred into a sealed 1.5-mL-capacity Eppendorf vial immersed in a microprocessor-controlled 280 Series digital water bath (Model 2837, Thermo Electron Corporation, OH, USA) set at 37 ± 0.5 °C. The time that elapsed for samples to stop flowing upon tube inversion was recorded using a West Bend electronic timer (West Bend Housewares LLC, WI, USA). In addition, tubes containing 500 μL of PBS were equilibrated to 37 ± 0.5 °C in the Thermo 2837 digital water bath, then injected with 200 μL SnPPIX-TIF, and the time to solidify was recorded. All measurements were performed in quadruplicate.

3.3.3. Particle Size and Polydispersity Index. Dynamic light scattering (DLS) was applied for mean hydrodynamic particle size and PDI quantifications using the Malvern Zetasizer (Malvern Instruments, Ltd., Malvern, U.K.). The particle size is a measure of particle diameter, while PDI quantifies the distribution of the particulate population.[41] Three independent SnPPIX-TIF samples were filled into separate disposable microcuvettes and analysis performed at 10 °C, using the Zetasizer.

3.4. Murine Animal Model. Male, 10−16-wk-old C57BL6 mice weighing 29.24 ± 3.89 g were obtained through a National Institute of Allergy and Infectious Diseases (NIAID) supply contract with Taconic Farms (Germantown, NY, USA). All animals used for *in vivo* studies were housed in Association for Assessment and Accreditation of Laboratory Animal Care International accredited biosafety level 2 (BSL 2) and level 3 (BSL 3) facilities at the NIAID, National Institutes of Health (NIH). Protocol (LPD-99E) approved by the NIAID Animal Care and Use Committee was employed for all *in vivo* experiments. Mice were contained under specific pathogen-free conditions, had ad libitum access to food and water, and were randomly grouped for the respective experiments.

3.5. In Vivo Injection Duration and Sol−Gel Transitioning. The average time required to inject SnPPIX-TIF or placebo-TIF preparations intramuscularly through a 25G needle into the right hind leg thighs of each mouse was measured utilizing a West Bend electronic timer. This experiment involved the use of two animal groups, where the first and second groups of uninfected mice (n = 5 in each case) received 0.1 mL of SnPPIX-TIF or placebo-TIF (control), respectively.

To visualize the sol−gel transitioning of the SnPPIX-TIF *in vivo* post-IM injection using a 25G needle equipped 1 mL syringe, three different sets of uninfected C57BL6 mice (n = 2) were studied. The first group consisted of animals that received 0.1 mL of SnPPIX-TIF at a dose of 5 mg/kg as an IM injection. The second set served as the secondary controls and received 0.1 mL of placebo-TIF via IM injection, while the third group received no treatment whatsoever (primary controls). The three mouse groups were sedated with inhalant 1.5%−2.0% isoflurane in a 50% oxygen gas mixture, using the PerkinElmer RAS-4 Rodent Anesthesia System; to aid visibility, all hair around both hind leg thighs was carefully shaved with electric clippers thereafter. Then, 0.1 mL of VivoTag 680 XL (a PerkinElmer Near-Infrared Fluorochrome Label) labeled placebo-TIF or SnPPIX-TIF (5 mg/kg) was injected intramuscularly into the right hind leg thighs of the second and third mouse groups, respectively. Post-injection, both treated and untreated mice were immediately transferred into the PerkinElmer IVIS Lumina LT Series III imaging platform (≤10 min) and then at 1, 4, and 24 h after injection. Precise noninvasive *in vivo* images were captured accordingly (after ∼1 min at 37 ± 0.1 °C for each time point), using the PerkinElmer Living Image software.

3.6. In Vivo Assay of Antitubercular Efficacy. *3.6.1. Mycobacterium tuberculosis Infections and Bacterial Load Quantification.* *Mycobacterium tuberculosis* (H37Rv strain) was maintained in 7H9 broth supplemented with 0.05% Tween 80 and 10% oleic acid−albumin-dextrose-catalase (OADC) at 37 °C. For efficacy studies, mice were infected with ∼100 CFU of the bacilli in an enclosed aerosol chamber (Glas Col, Terre Haute, IN, USA). For each infection performed, several mice (n = 5) were sacrificed after four weeks to determine initial bacterial uptake. Quantification of mycobacterial loads was performed by plating serial dilutions of lung tissue homogenates on agar plates composed of Middlebrook 7H11 supplemented with 0.5% v/v glycerol and 10% v/v OADC enrichment media. Bacterial colonies were enumerated 21 days post-incubation of the plates at 37 °C in a Thermo Scientific Environmental Chamber (Thermo Fisher Scientific−Asheville LLC, Marietta, OH, USA).

3.6.2. Drug Treatment and Sample Collection for Anti-TB Efficacy. Each *Mtb*-infected mouse received a 5 mg/kg SnPPIX treatment as IM or IP injection beginning at four weeks post-infection. The first mouse group (n = 5) was untreated and served as the control animals, the second group (n = 5) received SnPPIX-WBS IM daily, third set (n = 5) got SnPPIX-WBS IP daily, and the fourth group (n = 5) was treated with SnPPIX-TIF once weekly intramuscularly. An additional control group (n = 5) received placebo-TIF IM with the same 1 weekly dosing. All treatment schedules were executed over a total period of four weeks. Upon treatment completion, each animal was sacrificed and whole lung harvested into 1 mL sterile 1× DPBS solution for homogenization (Precellys Evolution Homogenizer, Bertin Corp., MD, USA). Bacterial load quantification was performed on serial dilutions of lung homogenates, as described above.

3.7. In Vivo Pharmacokinetic Studies. *3.7.1. Drug Treatment and Blood Collection.* To evaluate the impact of polymeric encapsulation of the *in vivo* kinetics of SnPPIX, uninfected mouse cohorts (n = 5 per experiment) were given one dose of 0.1 mL of SnPPIX-TIF or SnPPIX-WBS (5 mg/kg in both cases) by IM injection and blood samples collected over only 24 h. To further measure the pharmacokinetics of the newly developed SnPPIX-TIF, a 0.1 mL IM injection was administered once weekly for two weeks altogether, employing an additional mouse group (n = 5). All experimental animals were tail bled and 50−100 μL of blood collected into capillary tubes with push caps (Microvette CB 300 Potassium EDTA, Sarstedt AG and Co. KG, Nümbrecht, Germany) at predetermined time intervals for the respective experimental protocol. Plasma was isolated by centrifuging blood from each animal using the Soravll Legend Micro 17R centrifuge (Thermo Fisher Scientific, Waltham, MA, USA) set at 4 °C,

https://dx.doi.org/10.1021/acsptsci.0c00185
ACS Pharmacol. Transl. Sci. 2021, 4, 276−287

and 5000 rpm for 5 min. All plasma samples were stored at −80 °C for more quantitative analysis.

3.7.2. Plasma Sample Preparation and Drug Quantification. Frozen plasma samples were analyzed for SnPPIX blood levels at all scheduled time points using fluorometry. Briefly, 5−10 μL of plasma were used in the assay. If the volume of plasma was 5 μL, the final volume was adjusted to 10 μL with PBS. A quantity of 100 ng of deuteroporphyrin IX-2,4-disulfonic acid was added to each sample. This was followed by the addition of 35 μL of a solution consisting of 90% acetonitrile and 10% methanol, and 100 mM $HCl_{(MeOH)}$, which was then thoroughly mixed and allowed to stand for 5 min at room temperature. The samples were centrifuged (Eppendorf 5417R) for 10 min, at 18 000*g* at 10 °C. Next, the supernatant was transferred to fresh tubes and completely evaporated at 60 °C for 30 min in a centrifugal evaporator (LabConco Acid Resistant CentriVap). The residue was dissolved in 100 μL of an aqueous 25 mM 4-morpholine ethanesulfonic acid (MES), pH 6.0 and 50% dimethylformamide solution. The samples were read within 15 min in a Tecan M200 fluorescence plate reader (Tecan Group Ltd., Männedorf, Switzerland). The SnPPIX was detected at 407 nm excitation/585 nm emission and the internal standard, deuteroporphyrinIX-2,4-disulfonic acid, was detected at 407 nm excitation/695 nm emission. The calibration curves were prepared for each reading in 10 μL of plasma containing pure SnPPIX at concentrations from 5−600 ng and 100 ng of internal standard per standard. The curves were prepared in the same way and at the same time as the experimental samples. The ratios of SnPPIX fluorescence to that of the internal standard (10 data points per calibration) were fit to a polynomial (r^2 = 0.9997) to generate changes in the plasma concentration over time. Major pharmacokinetic parameters were computed using the GraphPad Prism version 7.04 software (GraphPad, San Diego, CA, USA).

3.8. Histopathology. For this study, uninfected animals were divided into groups (n = 3 for each assessment) that received 0.l mL of SnPPIX-TIF or 0.1 mL placebo-TIF weekly and, last, the untreated control animals. Drug-treated mice received 5 mg/kg SnPPIX and all injections were administered intramuscularly over a total of weeks. Multiple organs, including heart, kidney, lungs, liver, brain, testes, spleen, and injection site tissue (skeletal muscle), were collected from the different animal groups at the study end point and placed in 10% neutral-buffered formalin until adequately fixed. Thereafter, tissues were trimmed to a thickness of 3−5 mm, processed, and paraffin-embedded. The respective paraffin tissue blocks were sectioned at 5 μm and stained with H&E. Sections were examined by a board-certified veterinary pathologist, using an Olympus BX51 light microscope (Olympus Corporation, Tokyo, Japan) and photomicrographs were taken at magnifications of 4× and 20×, using an Olympus DP73 camera. Tissue sections were evaluated for the presence of histologic abnormalities (e.g., inflammation, necrosis, edema, fibrosis, vacuolation) and were individually scored using a standard lesion severity scale in which case 0 = no lesion, case 1 = minimal, case 2 = mild, case 3 = moderate, and case 4 = marked.[28]

3.9. Data Analysis. All data including graphical representations of findings are presented as mean ± standard deviation (SD). Sample size (n) is highlighted for each *in vivo* experiment, while *in vitro* evaluations are specified as the number of experimental replicates. All statistical and pharmacokinetic data analyses were executed by employing the GraphPad Prism version 7.04 software (GraphPad, San Diego, CA, USA). Test groups differences were comparatively analyzed using either the unpaired Student's *t*-test (for comparison between two data groups) or one or two-way analysis of variance (ANOVA). Statistical disparities were considered significant when $p \leq 0.05$ ((*) $p \leq 0.05$, (**) $p \leq 0.01$, (***) or (****) $p \leq 0.0001$).

4. CONCLUSIONS

The encapsulation of drug molecules into extended-release polymer-based thermoresponsive matrices can improve the duration of therapeutic action after a single-dose injection. Here, we report the development of a biocompatible, sustained release intramuscular (IM) injection loaded with tin protoporphyrin (SnPPIX), a heme oxygenase-1 inhibitor recently shown to have efficacy in a murine experimental model as a host directed therapeutic agent for pulmonary tuberculosis. Previously, it was administered as multiple daily intraperitoneal (IP) aqueous injections, which would be impractical for human use. Hence, the development of a polymeric carrier for SnPPIX IM delivery once weekly represents an important advance in making this therapy clinically feasible. The SnPPIX thermoresponsive injectable formulation (SnPPIX-TIF) that we describe was found to be microparticulate, easily injectable and syringeable, physicochemically stable, and formed solid, drug-releasing gels under both *in vitro* biorelevant and *in vivo* physiological conditions. In addition, we obtained experimental evidence that SnPPIX-TIF is well-tolerated *in vivo* and maintains higher therapeutically effective drug plasma levels over an extended period, compared to the conventional aqueous SnPPIX IP or IM administered formulations. Our findings thus support the general use of thermoresponsive polymer-based carriers as robust drug delivery systems for the management of other ailments, in addition to tuberculosis. To confirm this applicability, a broad range of therapeutic agents would have to be investigated, integrated into the carrier matrix, and tested to determine whether they achieve the desired pharmacotherapeutic outcomes. In the case of TB, the observations reported here make the long-acting thermoresponsive formulation we have devised attractive for flexible, staggered dosing and better patient compliance, which are both important for effective treatment of this disease. Critical next steps will be to comprehensively evaluate and modify SnPPIX-TIF physicochemical properties to further optimize and sustain its *in vivo* drug release/absorption capabilities and assess its treatment shortening performance as an adjunct to conventional tuberculosis chemotherapy, as well as examine its efficacy and safety in additional animal models.

AUTHOR INFORMATION

Corresponding Author

Oluwatoyin A. Adeleke − *Immunobiology Section, Laboratory of Parasitic Diseases, National Institute of Allergy and Infectious Diseases, National Institutes of Health, US Department of Health and Human Services, Bethesda, Maryland 20892, United States; Division of Pharmaceutical Sciences, School of Pharmacy, Sefako Makgatho Health Science University, Pretoria 0208, South Africa;* orcid.org/0000-0002-0880-3997; Email: oluwatoyin.adeleke@fulbrightmail.org; Fax: +1 202 604 4884

https://dx.doi.org/10.1021/acsptsci.0c00185
ACS Pharmacol. Transl. Sci. 2021, 4, 276−287

Authors

Logan Fisher − *Immunobiology Section, Laboratory of Parasitic Diseases, National Institute of Allergy and Infectious Diseases, National Institutes of Health, US Department of Health and Human Services, Bethesda, Maryland 20892, United States*

Ian N. Moore − *Infectious Disease Pathogenesis Section (IDPS), Comparative Medicine Branch, National Institute of Allergy and Infectious Diseases, National Institutes of Health, US Department of Health and Human Services, Rockville, Maryland 20852, United States*

Glenn A. Nardone − *Protein Chemistry Section, Research Technologies Branch, National Institute of Allergy and Infectious Diseases, National Institutes of Health, US Department of Health and Human Services, Rockville, Maryland 20852, United States*

Alan Sher − *Immunobiology Section, Laboratory of Parasitic Diseases, National Institute of Allergy and Infectious Diseases, National Institutes of Health, US Department of Health and Human Services, Bethesda, Maryland 20892, United States*

Complete contact information is available at: https://pubs.acs.org/10.1021/acsptsci.0c00185

Author Contributions

Conceptualization was done by O.A.A. and A.S. Study design was performed by O.A.A.; the methodology was derived by O.A.A., L.M.F., G.A.N., and I.N.M. Investigation was performed by O.A.A., L.M.F., G.A.N., and I.N.M. Data analysis was performed by O.A.A., I.N.M., G.A.N.; resources were the responsibility of O.A.A., I.N.M., G.A.N., and A.S. Histopathological analysis and interpretation was performed by I.N.M. Plasma sample preparation and drug quantification was executed by G.A.N. Funding acquisition was done by O.A.A. and A.S., whereas validation was done by O.A.A., L.M.F., G.A.N., and I.N.M. Project administration was orchestrated by O.A.A. and A.S. The original draft was written by O.A.A., and the review and editing was done by O.A.A., L.M.F., G.N., I.N.M., and A.S. All authors read and approved the published version of the manuscript.

Funding

Research reported in this publication was funded through grant support from the US−South Africa Program for Collaborative Biomedical Research, under Award No. U01AI115940. Additional funding was provided by the Division of Intramural Research Program, National Institute of Allergy and Infectious Diseases, National Institute of Health; the Division of Research Capacity Development (Staff Development Grant Programme), South African Medical Research Council and Sefako Makgatho Health Sciences University, South Africa. The content is solely the responsibility of the authors and does not necessarily represent the official views of the funders.

Notes

The authors declare no competing financial interest.

■ ACKNOWLEDGMENTS

The authors thank Drs. David Garboczi, Gittis Apostolos (Structural Biology Section), and Jeffery Americo (Laboratory for Viral Diseases), National Institute of Allergy and Infectious Diseases (NIAID), National Institute of Health (NIH) for access to their technical expertise, equipment, and useful discussions. We are most thankful for the technical assistance provided by Sandy Oland, Virgilio Bundoc, and the staff of the Animal Care Facility, Comparative Medicine Branch, Building 33, NIAID, NIH. Also, we are grateful to Prof. Robert Wilkinson, Drs. Yolande Harley (University of Cape Town), Véronique Dartois (Hackensack Meridian Health Center for Discovery and Innovation), Dragana Jankovic, Helena Boshoff, Diego Costa, Eduardo Amaral, Sivaranjani Namasivayam, and Sanjay Gautam (NIAID, NIH) for their valuable input.

■ REFERENCES

(1) Smith, I. (2003) Mycobacterium tuberculosis pathogenesis and molecular determinants of virulence. *Clin. Microbiol. Rev. 16* (3), 463−496.

(2) Jordao, L., and Vieira, O. V. (2011) Tuberculosis: new aspects of an old disease. *Int. J. Cell Biol. 2011*, 1.

(3) Pezzella, A. T. (2019) History of Pulmonary Tuberculosis. *Thoracic Surgery Clinics 29* (1), 1−17.

(4) Hussain, A., Shakeel, F., Singh, S. K., Alsarra, I. A., Faruk, A., Alanazi, F. K., and Christoper, G. V. P. (2019) Solidified SNEDDS for the oral delivery of rifampicin: Evaluation, proof of concept, in vivo kinetics, and in silico GastroPlusTM simulation. *Int. J. Pharm. 566*, 203−217.

(5) Ionescu, A. M., Mpobela Agnarson, A., Kambili, C., Metz, L., Kfoury, J., Wang, S., Williams, A., Singh, V., and Thomas, A. (2018) Bedaquiline-versus injectable-containing drug-resistant tuberculosis regimens: a cost-effectiveness analysis. *Expert Review of Pharmacoeconomics and Outcomes Research 18* (6), 677−689.

(6) MacNeil, A., Glaziou, P., Sismanidis, C., Date, A., Maloney, S., and Floyd, K. (2020) Global epidemiology of tuberculosis and progress toward meeting global targets — Worldwide, 2018. *Morbidity and Mortality Weekly Report 69*, 281−285.

(7) World Health Organization (WHO). *Global Tuberculosis Report* (2020). Available at: https://apps.who.int/iris/bitstream/handle/10665/336069/9789240013131-eng.pdf?ua=1 (accessed Oct. 28, 2020).

(8) *TB Alliance* (2019). Available via the Internet at: https://www.tballiance.org/why-new-tb-drugs/global-pandemic (accessed Oct. 2, 2020).

(9) Adeleke, O. A., Tsai, P. C., Karry, K. M., Monama, N. O., and Michniak-Kohn, B. B. (2018) Isoniazid-loaded orodispersible strips: Methodical design, optimization and in vitro-in silico characterization. *Int. J. Pharm. 547* (1−2), 347−359.

(10) Verma, M., Vishwanath, K., Eweje, F., Roxhed, N., Grant, T., Castaneda, M., Steiger, C., Mazdiyasni, H., Bensel, T., Minahan, D., et al. (2019) A gastric resident drug delivery system for prolonged gram-level dosing of tuberculosis treatment. *Sci. Transl. Med. 11* (483), eaau6267.

(11) World Health Organization. *Treatment of Tuberculosis: Guidelines—4th Edition* (2010). Available via the Internet at: http://apps.who.int/iris/bitstream/handle/10665/44165/9789241547833_eng.pdf (accessed Oct. 13, 2020).

(12) Karumbi, J., and Garner, P. (2015) Directly observed therapy for treating tuberculosis. *Cochrane Database Syst. Rev.* No. 5, CD003343.

(13) Steffen, R., Menzies, D., Oxlade, O., Pinto, M., de Castro, A. Z., Monteiro, P., and Trajman, A. (2010) Patients' costs and cost-effectiveness of tuberculosis treatment in DOTS and non-DOTS facilities in Rio de Janeiro, Brazil. *PLoS One 5* (11), e14014.

(14) Kolloli, A., and Subbian, S. (2017) Host-directed therapeutic strategies for tuberculosis. *Front. Med. 4*, 171.

(15) Liu, Q., Abba, K., Alejandria, M. M., Sinclair, D., Balanag, V. M., and Lansang, M. A. D. (2014) Reminder systems to improve patient adherence to tuberculosis clinic appointments for diagnosis and treatment. *Cochrane Database Syst. Rev.* No. 11, CD006594.

(16) Lutge, E. E., Wiysonge, C. S., Knight, S. E., Sinclair, D., and Volmink, J. (2015) Incentives and enablers to improve adherence in tuberculosis. *Cochrane Database Syst. Rev.* No. 9, CD007952.

(17) Prasad, R., Gupta, N., and Banka, A. (2017) Rapid diagnosis and shorter regimen for multidrug-resistant tuberculosis: A priority to

improve treatment outcome. *Lung India: Off. Organ Indian Ches Soc. 34* (1), 1−2.
(18) Wallis, R. S., and Hafner, R. (2015) Advancing host-directed therapy for tuberculosis. *Nat. Rev. Immunol. 15* (4), 255−263.
(19) Costa, D. L., Namasivayam, S., Amaral, E. P., Arora, K., Chao, A., Mittereder, L. R., Maiga, M., Boshoff, H. I., Barry, C. E., Goulding, C. W., and Andrade, B. B. (2016) Pharmacological inhibition of host heme oxygenase-1 suppresses Mycobacterium tuberculosis infection in vivo by a mechanism dependent on T lymphocytes. *mBio 7* (5), e01675-16.
(20) Dutta, N. K., Bruiners, N., Zimmerman, M. D., Tan, S., Dartois, V., Gennaro, M. L., and Karakousis, P. C. (2020) Adjunctive host-directed therapy with statins improves tuberculosis-related outcomes in mice. *J. Infect. Dis. 221*, 1079.
(21) Young, C., Walzl, G., and Du Plessis, N. (2020) Therapeutic host-directed strategies to improve outcome in tuberculosis. *Mucosal Immunol. 13*, 190.
(22) Pibiri, M., Leoni, V. P., and Atzori, L. (2018) Heme oxygenase-1 inhibitor tin-protoporphyrin improves liver regeneration after partial hepatectomy. *Life Sci. 204*, 9−14.
(23) Abdalla, M. Y., Ahmad, I. M., Rachagani, S., Banerjee, K., Thompson, C. M., Maurer, H. C., Olive, K. P., Bailey, K. L., Britigan, B. E., and Kumar, S. (2019) Enhancing responsiveness of pancreatic cancer cells to gemcitabine treatment under hypoxia by heme oxygenase-1 inhibition. *Translational Research 207*, 56−69.
(24) Chowdhury, M. A., Choi, M., Ko, W., Lee, H., Kim, S. C., Oh, H., Woo, E. R., Kim, Y. C., and Lee, D. S. (2019) Standardized microwave extract of Sappan Lignum exerts anti-inflammatory effects through inhibition of NF-κB activation via regulation of heme oxygenase-1 expression. *Mol. Med. Rep. 19* (3), 1809−1816.
(25) El-Achkar, G. A., Mrad, M. F., Mouawad, C. A., Badran, B., Jaffa, A. A., Motterlini, R., Hamade, E., and Habib, A. (2019) Heme oxygenase-1-Dependent anti-inflammatory effects of atorvastatin in zymosan-injected subcutaneous air pouch in mice. *PLoS One 14* (5), No. e0216405.
(26) Turner, P. V., Brabb, T., Pekow, C., and Vasbinder, M. A. (2011) Administration of substances to laboratory animals: routes of administration and factors to consider. *J. Am. Assoc. Lab. Animal Sci. 50* (5), 600−613.
(27) Al Shoyaib, A., Archie, S. R., and Karamyan, V. T. (2020) Intraperitoneal Route of Drug Administration: Should it Be Used in Experimental Animal Studies? *Pharm. Res. 37* (1), 12.
(28) Risselada, M., Linder, K. E., Griffith, E., Roberts, B. V., Davidson, G., Zamboni, W. C., and Messenger, K. M. (2017) Pharmacokinetics and toxicity of subcutaneous administration of carboplatin in poloxamer 407 in a rodent model pilot study. *PLoS One 12* (10), No. e0186018.
(29) de Souza Ferreira, S. B., Braga, G., Oliveira, É.L., da Silva, J. B., Rosseto, H. C., de Castro Hoshino, L. V., Baesso, M. L., Caetano, W., Murdoch, C., Colley, H. E., and Bruschi, M. L. (2019) Design of a nanostructured mucoadhesive system containing curcumin for buccal application: from physicochemical to biological aspects. *Beilstein J. Nanotechnol. 10* (1), 2304−2328.
(30) Moura, S., Noro, J., Cerqueira, P., Silva, C., Cavaco-Paulo, A., and Loureiro, A. (2020) Poloxamer 407 based-nanoparticles for controlled release of methotrexate. *Int. J. Pharm. 575*, 118924.
(31) Russo, E., and Villa, C. (2019) Poloxamer Hydrogels for Biomedical Applications. *Pharmaceutics 11* (12), 671.
(32) Sharma, M., and Mehta, I. (2019) Surface stabilized atorvastatin nanocrystals with improved bioavailability safety and antihyperlipidemic potential. *Sci. Rep. 9* (1), 16105.
(33) Kadajji, V. G., and Betageri, G. V. (2011) Water soluble polymers for pharmaceutical applications. *Polymers 3* (4), 1972−2009.
(34) Boonlai, W., Tantishaiyakul, V., Hirun, N., Sangfai, T., and Suknuntha, K. (2018) Thermosensitive Poloxamer 407/poly (acrylic acid) hydrogels with potential application as injectable drug delivery system. *AAPS PharmSciTech 19* (5), 2103−2117.
(35) Schmolka, I. R. (1972) Artificial skin I. Preparation and properties of pluronic F-127 gels for treatment of burns. *J. Biomed. Mater. Res. 6* (6), 571−582.
(36) Sherif, S., Bendas, E. R., and Badawy, S. (2014) The clinical efficacy of cosmeceutical application of liquid crystalline nano-structured dispersions of alpha lipoic acid as anti-wrinkle. *Eur. J. Pharm. Biopharm. 86* (2), 251−259.
(37) Liu, C., Wu, J., Gan, D., Li, Z., Shen, J., Tang, P., Luo, S., Li, P., Lu, X., and Zheng, W. (2020) The characteristics of mussel-inspired nHA/OSA injectable hydrogel and repaired bone defect in rabbit. *J. Biomed. Mater. Res., Part B 108*, 1814.
(38) Zhang, Q., Fassihi, M. A., and Fassihi, R. (2018) Delivery Considerations of Highly Viscous Polymeric Fluids Mimicking Concentrated Biopharmaceuticals: Assessment of Injectability *via* Measurement of Total Work Done "W_T". *AAPS PharmSciTech 19* (4), 1520−1528.
(39) Watt, R. P., Khatri, H., and Dibble, A. R. (2019) Injectability as a function of viscosity and dosing materials for subcutaneous administration. *Int. J. Pharm. 554*, 376−386.
(40) Cilurzo, F., Selmin, F., Minghetti, P., Adami, M., Bertoni, E., Lauria, S., and Montanari, L. (2011) Injectability evaluation: an open issue. *AAPS PharmSciTech 12* (2), 604−609.
(41) Murgia, D., Angellotti, G., D'Agostino, F., and De Caro, V. (2019) Bioadhesive Matrix Tablets Loaded with Lipophilic Nano-particles as Vehicles for Drugs for Periodontitis Treatment: Development and Characterization. *Polymers 11* (11), 1801.
(42) Alcantara, K. P., Zulfakar, M. H., and Castillo, A. L. (2019) Development, characterization and pharmacokinetics of mupirocin-loaded nanostructured lipid carriers (NLCs) for intravascular administration. *Int. J. Pharm. 571*, 118705.
(43) Simon, A., de Almeida Borges, V. R., Cabral, L. M., and de Sousa, V. P. (2013) Development and validation of a discriminative dissolution test for betamethasone sodium phosphate and betame-thasone dipropionate intramuscular injectable suspension. *AAPS PharmSciTech 14* (1), 425−434.
(44) Peltonen, L. (2018) Practical guidelines for the characterization and quality control of pure drug nanoparticles and nano-cocrystals in the pharmaceutical industry. *Adv. Drug Delivery Rev. 131*, 101−115.
(45) Nardi-Ricart, A., Nofrerias-Roig, I., Suñé-Pou, M., Pérez-Lozano, P., Miñarro-Carmona, M., García-Montoya, E., Ticó-Grau, J. R., Insa Boronat, R., and Suñé-Negre, J. M. (2020) Formulation of Sustained Release Hydrophilic Matrix Tablets of Tolcapone with the Application of Sedem Diagram: Influence of Tolcapone's Particle Size on Sustained Release. *Pharmaceutics 12* (7), 674.

https://dx.doi.org/10.1021/acsptsci.0c00185
ACS Pharmacol. Transl. Sci. 2021, 4, 276−287